



Cite this: *CrystEngComm*, 2023, 25, 6472

Structural features that modulate the sharpness of the spin crossover transition in $[\text{Fe}^{\text{III}}(5\text{-X-qsal})_2]^+$ based salts†

Bruno J. C. Vieira, * Laura C. J. Pereira, * Vasco da Gama and João C. Waerenborgh

This study aimed to unveil the structural modifications that can modulate the SCO transition sharpness, occurring up to room temperature, of Fe^{III} compounds with general formula $[\text{Fe}(5\text{-X-qsal})_2]^+$. These compounds are organized in layers of cationic chains. The structure of a series of compounds with different transition progressions were analyzed and compared to extract the structural differences responsible for the change in magnetic behavior. Two structural differences were found to be responsible for the modulation of the magnetic transition sharpness, in direct correspondence with the degree of interactions between the cations in each chain and between chains. The reinforcement of the interchain connectivity was found to contribute towards the sharpness of the transition. On the contrary, the reinforcement of the interlayer interactions resulted in the broadening of the transition. To achieve sharp transitions, it is necessary to obtain structures able to maximize interchain cation–cation interactions at the same time as they minimize the interlayer interactions.

Received 27th September 2023,
Accepted 3rd November 2023

DOI: 10.1039/d3ce00954h

rsc.li/crystengcomm

Introduction

Spin crossover (SCO) is one of the most exciting examples of switching ability in molecular materials. Complexes with octahedral coordination geometry and a central metal atom with $3d^n$ ($4 \leq n \leq 7$) electronic configuration are known to be able to show a crossover between a low-spin (LS) and a high-spin (HS) state.¹ This SCO may be achieved by submitting these materials to external perturbations such as temperature, pressure, magnetic field and light irradiation. The electronic transition in the system is followed by changes in their physical properties (colour, magnetism, crystal structure) that are able to be monitored by a variety of different techniques.^{1–3} The transition can exhibit different dynamics involving its rate (gradual *vs.* sharp), its completeness (complete *vs.* incomplete), the number of steps (single step *vs.* multi-step), and can even exhibit hysteresis.^{1–3} The modulation of the transition dynamics is correlated to the mechanism of propagation of the SCO transition through the solid structure, *i.e.*, the degree of cooperativity between the SCO centers. This cooperativity

can be defined as the efficiency with which the sum of all the supramolecular interactions existing in each solid structure is able to propagate the SCO transition. The cooperativity level can be drastically altered by the modification of the number of supramolecular interactions or by modifying the type, such as hydrogen⁴ or halogen bonding,⁵ or π – π stacking.⁶

Although difficult, it is possible to identify the interactions responsible for the control of specific mechanisms of the spin transition. In previous work,⁷ we were able to identify in a series of Fe^{III} compounds, three supramolecular arrangements correlated to different magnetic behaviors, one of them exhibiting a spin transition in the temperature range between 4 K and room temperature. In this work we expand that study and identify the structural interaction and supramolecular features that modulate the shape of the transition in these SCO compounds. This information is critical towards the intelligent design of SCO materials as it enables the targeted synthesis of compounds with a desired transition morphology (sharp or gradual). To unveil these key interactions a series of compounds with similar composition exhibiting SCO with different transition shapes were analyzed. Their structural features were compared in order to extract patterns associable to differences in the SCO transition sharpness. We have analyzed compounds based on *N*-(8-quinolyl)salicylaldimine (qsal, Fig. 1), namely a series of Fe^{III} SCO complexes with general formula $[\text{Fe}(5\text{-X-qsal})_2]^+$ reported in the literature, which exhibit reversible SCO

Centro de Ciências e Tecnologias Nucleares, DECN, Instituto Superior Técnico, Universidade de Lisboa, E.N. 10, km 139.7, 2695-066 Bobadela LRS, Portugal.

E-mail: brunovieira@ctn.tecnico.ulisboa.pt, lpereira@ctn.tecnico.ulisboa.pt

† Electronic supplementary information (ESI) available. See DOI: <https://doi.org/10.1039/d3ce00954h>



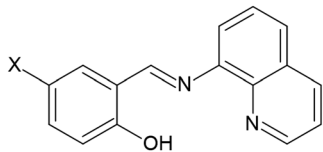


Fig. 1 Qsal ligand.

transition with various degrees of transition sharpness. Their magnetic properties were correlated with the structural data extracted from single crystal X-ray diffraction.

Hereafter the reference to the compounds will have one of the following numerical prefixes depending on X, 1 (X=H), 2 (X=Cl), 3 (X=Br), 4 (X=I) and 5 (X=OCH₃). As an example, the compound with formula [Fe(5-I-qsal)₂]PF₆·1.5H₂O will be referred to as **4-PF₆·1.5H₂O**.

Complexes coupled with transition metal anions such as dithiolates like [Ni(dmit)₂][−] (dmit = 4,5-dithiolato-1,3-dithiole-2-thione) were excluded from this study due to their disparity of supramolecular arrangements arising from the ease with which they create segregated layers of highly connected anions. These materials are expected to have different supramolecular arrangements than the compounds addressed in the present study.

Results and discussion

As mentioned in a previous work,⁷ compounds derived from the cations with general formula [Fe(5-X-qsal)₂]⁺, exhibiting SCO up to room temperature, have the same overall supramolecular arrangement. In these salts where the [Fe(5-X-qsal)₂]⁺ cations are essentially in the HS configuration at room temperature, the difference in the progress of the SCO transition observed is due to slight differences in the otherwise strong cooperativity between the cations in these systems. These compounds share the same structural motive (that we named chain layers in the previous work⁷) consisting of arrangements of parallel layers of chains of cations leading to a supramolecular configuration consistent with layers of cation chains. Within these chains, the cations display very strong intrachain cation–cation (hereafter called DD) interactions resulting from the overlap of the 5-X-qsal fragments extending through the entire ligands. Short CH⋯O contacts and even C–X⋯π type II halogen bond contacts reinforce the strong ππ interactions. These intrachain interactions are the strongest in all the studied compounds with little to no difference detected among them. Two other types of supramolecular interactions are also present in these structures: interactions between chains in the same layer (interchain interactions) and interactions between chains of adjacent layers (interlayer interactions). The interchain interactions consist in relatively strong DD interactions, mostly associated with close contacts between the quinoline (Qn) fragments of cations located in neighboring chains, with no assistance from solvent or anion molecules. The interlayer interactions are the weakest type of

interaction present in these structures, being composed of DD interactions that are commonly reinforced by cation–anion–cation (hereafter DAD) connectivity. In summary the chain layers structural motive consists in cationic chains with significant intrachain and interchain DD interactions but weaker interlayer interactions (Fig. S1†). This combination of interactions allows for a relatively rigid layer of cations, which can induce easy propagation of the lattice distortions and SCO processes but with various degrees of sharpness. The in-depth analysis of this structural motive can be found in the previous work.⁷

We observed that in this family of compounds, that undergo spin transition up to room temperature, although the intrachain interactions appear to be always the same, and always the strongest of the structure, the interchain and interlayer interactions exhibited a noticeable difference in both quantity and type of interactions. In order to determine how these structural differences could influence the progression of the SCO transition we selected to study 13 of these compounds with reversible spin transition but different transition progression. In order to organize the discussion below, these compounds were divided into two types based in the temperature range of the transition (ΔT): sharp transition (Sh) corresponding to compounds with 4 K < ΔT < 50 K and gradual transition (Gr) corresponding to compounds with ΔT > 50 K. The value of 50 K was chosen by the authors of this study taking into account the values of ΔT (Table 1) in conjunction with the structural features exhibited by the compounds in this study. The selected compounds for this study are **1-I₃** (Gr),⁸ **1-SCN** (Sh, Sh),⁹ **1-SeCN** (Sh, Sh),¹⁰ **2-SCN·MeOH** (Gr, Sh),¹¹ **2-PF₆·MeCN** (Sh),⁷ **3-NO₃·2MeOH** (Sh, Sh),¹² **3-PF₆·H₂O** (Gr),⁷ **4-CF₃SO₃·*n*PrOH** (Gr),¹³ **4-CF₃SO₃·*i*PrOH** (Gr),¹³ **4-CF₃SO₃·MeOH** (Sh),¹⁴ **4-PF₆·1.5H₂O** (Sh),⁷ **4-N(SO₂CF₃)₂** (Sh)¹⁵ and **5-Cl·MeCN·H₂O** (Sh, Sh).¹⁶ A summary of the magnetic and structural information of these compounds can be found in Table 1.

In the case of the analysis of the interchain interactions it is possible to extract a numeric value that can be associate to the degree of interaction of cation, because they have their Qn fragments parallel to each other and this distance correlates well with the degree of interactions present in each structure. Unfortunately it is impossible to obtain a similar numeric parameter for the interlayer connectivity. In this case there are different types of interactions that contribute to the overall connectivity (DD and DAD). Furthermore the DAD interactions involve different atoms (with different atomic and ionic rays) in each structure, making it impossible to calculate a structural distance or short-contact value able to correlate with the observed degree of interaction. In compounds where we report differences in these interactions we will provide structural images that justify our statements.

The selected compounds for this study with a transition temperature range larger than 50 K, *i.e.* ΔT > 50 K (referred to as gradual Gr in this study) are **1-I₃** (Gr),⁸ **2-SCN·MeOH** (Gr, Sh),¹¹ **3-PF₆·H₂O** (Gr),⁷ **4-CF₃SO₃·*n*PrOH** (Gr)¹³ and **4-CF₃SO₃·*i*PrOH** (Gr).¹³



Table 1 Relevant structural and magnetic data for **1-I₃**, **1-SCN**, **1-SeCN**, **2-SCN·MeOH**, **2-PF₆·MeCN**, **3-NO₃·2MeOH**, **3-PF₆·H₂O**, **4-CF₃SO₃·*n*PrOH**, **4-CF₃SO₃·*i*PrOH**, **4-CF₃SO₃·MeOH**, **4-PF₆·1.5H₂O**, **4-N(SO₂CF₃)₂** and **5-Cl·MeCN·H₂O**

Compound	SCO step	Structure temperature/spin state	SCO type ^a (ΔT)	$T_{1/2}$ (K)	Inter-chain DD distance ^b (Å)	Ref.
1-I₃	1 step	50 K/LS	Gr (69 K)	240	3.422	8
1-SCN	2 steps	RT/HS	Sh (25 K)	203 [↓] , 290 [↑]	3.688	9
		RT/HS	Sh (25 K)	203 [↓] , 210 [↑]	3.688	
1-SeCN	2 steps	RT/HS	Sh (10 K)	212 [↓] , 282 [↑]	3.648	10
		RT/HS	Sh (10 K)	212 [↓] , 215 [↑]	3.648	
2-SCN·MeOH	2 steps	100 K/LS	Gr (73 K)	250	3.891	12
		100 K/LS	Sh (40 K)	167 [↓] , 177 [↑]	3.891	
2-PF₆·MeCN	1 step	150 K/LS	Sh (44 K)	265	3.445	7
3-NO₃·2MeOH	2 steps	123 K/LS	Sh (13 K)	229 [↓] , 234 [↑]	3.285	12
		123 K/LS	Sh (12 K)	128 [↓] , 144 [↑]	3.285	
3-PF₆·H₂O	1 step	150 K/LS	Gr (60 K)	220	3.380	7
4-CF₃SO₃·<i>n</i>PrOH	1 step	100 K/LS	Gr (64 K)	199	3.091	13
4-CF₃SO₃·<i>i</i>PrOH	1 step	163 K/LS	Gr (96 K)	251	3.091	13
4-CF₃SO₃·MeOH	1 step	163 K/LS	Sh (8 K)	232 [↓] , 234 [↑]	3.371	14
4-PF₆·1.5H₂O	1 step	150 K/LS	Sh (4 K)	268 [↓] , 272 [↑]	3.350	7
4-N(SO₂CF₃)₂	1 step	245 K/LS	Sh (34 K)	244 [↓] , 278 [↑]	3.336	15
5-Cl·MeCN·H₂O	2 steps	100 K/LS	Sh (21 K)	270	3.330	16
		100 K/LS	Sh (12 K)	240	3.330	

$T_{1/2}$ temperature calculated as the maximum of the first derivative $d\chi T/dT$. If $T_{1/2}$ observed when T decreases ↓ and when T increases ↑ are different, there is hysteresis. ^a Type of transition and degree of cooperativity (Gr-gradual, Sh-sharp). The value between brackets (ΔT ; in K) corresponds to the estimated span of the HS → LS transition, considering the slope of $d\chi T/dT$ at $T_{1/2}$ and extrapolating it to the χT^{HS} and χT^{LS} limits. There are two ΔT values when SCO takes place in two steps. ^b Distance between the planes formed by the Qn fragments of cations in neighboring chains of the same layer.

4-CF₃SO₃·*n*PrOH (Gr)¹³ and **4-CF₃SO₃·*i*PrOH** (Gr)¹³ exhibit crystal structures also quite similar to Sh compounds such as **1-SCN**, **1-SeCN**, **4-CF₃SO₃·MeOH** or **4-PF₆·1.5H₂O**. This is even reinforced by the values of the interchain DD distances presented in Table 1, where **4-CF₃SO₃·*n*PrOH** (Gr)¹³ and **4-CF₃SO₃·*i*PrOH** (Gr)¹³ exhibit the lowest values of all compounds. In these salts, however, the interchain interactions between the two quinoline, Qn, fragments are expected to be considerably weaker when compared with Sh compounds, due to a much poorer overlap between the aromatic fragments of the interacting ligands, which is expected to lead to softer cationic layers and less overall cooperative SCO behaviour (Fig. S2†).

This effect is less pronounced for **4-CF₃SO₃·*n*PrOH**, as in this case there are still relatively weak $\pi\pi$ interactions between the Qn fragments, which results in a faster rise of χT in the SCO process of this salt. In summary for **4-CF₃SO₃·*n*PrOH** (Gr)¹³ and **4-CF₃SO₃·*i*PrOH** (Gr)¹³ the structural difference related to the softer transition is the lower degree of interchain connectivity between cations within the same layer.

For **3-PF₆·H₂O** (Gr),⁷ the only structural difference observed when compared with compounds that exhibit a lower temperature range of the transition is the DAD interlayer interactions, which assist the DD interlayer connectivity. In this compound the effect of the cation–anion (hereafter DA) interactions is expected to be slightly enhanced, as in this salt there are two anions contributing to the reinforcement of DD interlayer interactions. Furthermore, the anions establish an additional DAD interaction to a second cation located in the neighbouring layer, reinforcing

the overall interlayer connectivity (b and e in Fig. S3†). In a similar fashion in **1-I₃** (Gr)⁸ the only difference regarding supramolecular arrangement or interactions, that could be associated with the reduction in the sharpness of the SCO process, is the existence of significant interlayer connectivity provided by the DAD interactions, as the I₃[−] anions seem to be particularly effective in the indirect interlayer connectivity (Fig. S4†). In both cases, the reduction of sharpness of the transition is originated in the reinforcement of the interlayer connectivity.

The **2-SCN·MeOH** (Gr, Sh)¹¹ structure, presents slightly weaker interchain contacts between the Ph–X groups that are established between each cation and two cations located in adjacent chains of the same layer. These DD intrachain interactions consist in a combination involving $\pi\pi$ contacts between the Ph groups and two-fold CCl $\cdots\pi$ contacts. In this case, the larger separation of the Ph groups (3.891 Å) when compared to the separation of the Qn groups in the other salts (ranging from 3.285 to 3.422 Å in compounds with Sh transition and structures in the LS state), suggests that these interactions must be weaker. As in the other Sh salts, only relatively weak interlayer DD interactions (CH $\cdots\pi$ contacts) are observed with interatomic distances of the order of the sum of the van der Waals radii. The reduction of the cooperativity of the SCO processes in **2-SCN·MeOH** can only be associated to the lower rigidity (softer interchain interactions) expected for the cationic layer.

The analysis of the structure of the five compounds with gradual transitions indicates that there are two different structural modifications responsible for the loss of sharpness of the transition (decrease of cooperativity): lower degree of



DD interchain connectivity or higher DD interlayer connectivity. The increase of the interlayer connectivity may arise in two different ways, directly through DD interlayer connectivity or through the assistance of the anion with the appearance of DAD. The structures analysed in this study do not allow determining if any of these sources of the enhancement of the interlayer connectivity (direct DD or assisted DAD) can have a greater impact in the loss of cooperativity. As far as this study could analyse, both have the same impact in the loss of cooperativity of the compound.

It is important to mention that the interchain interactions do not have to correlate directly with the size of the ligands. The increase in the atomic volume of ligands does not necessarily lead to a decrease of the cooperativity of the compound. This is evidenced by the comparison of, **2-PF₆·MeCN** (Sh), **3-PF₆·H₂O** (Gr) and **4-PF₆·1.5H₂O** (Sh)⁷ (Fig. 2). These compounds share the same anion and only differ in the halogen substitution (Cl, Br, and I respectively) and the solvating molecule. One might expect that the difference between the SCO progressions would be originated at least in part by the distinct interchain interactions originated in the dissimilar ligand volume due to the halogen atom used in each compound. The analysis of the SCO transition reveals however a different case. The sharpest transition, $\Delta T = 4$ K, is exhibited by **4-PF₆·1.5H₂O** with the bulkiest halogen atom in the ligand. Moreover, the second sharpest transition, $\Delta T = 44$ K, is exhibited by **2-PF₆·MeCN** with the smallest halogen. **3-PF₆·H₂O**, with the halogen substitute with the intermediate volume, exhibits the more gradual transition, $\Delta T = 60$ K. In these compounds the progression of the transition is not the result of differences in the interchain interactions since they are all very similar in all three compounds.

The major structural differences are associated with the variations in the interlayer connectivity, resulting either from the direct DD contacts or from the indirect connectivity mediated by the anions (Fig. S3†).

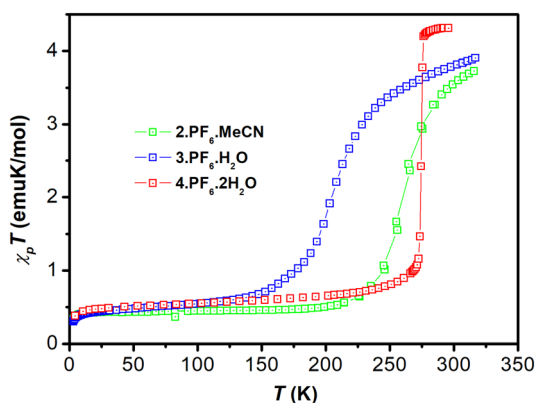


Fig. 2 Temperature dependence of $\chi_p T$ product in a field of 1 T of **2-PF₆·MeCN**, **3-PF₆·H₂O** and **4-PF₆·1.5H₂O**. Data reported in ref. 7.

The major difference in the direct DD interlayer connectivity concerns the stronger interactions that are observed for **2-PF₆·MeCN**, where DD interlayer interactions, associated with the two-fold $\text{CH}\cdots\pi$ contacts, seem to be stronger than the corresponding interactions in the other two salts. A larger variability is found for the indirect DAD interlayer connectivity reinforcing the direct DD interlayer connectivity. This connectivity is expected to be significantly stronger in the case of **3-PF₆·H₂O** than in **2-PF₆·MeCN** and to be the weakest for **4-PF₆·1.5H₂O**, which correlates quite well with the observed increase in the cooperativity of the SCO processes.

The analysis of the structures of the compounds with sharp transitions (**1·SCN** (Sh, Sh),⁹ **1·SeCN** (Sh, Sh),¹⁰ **2-PF₆·MeCN** (Sh),⁷ **3·NO₃·2MeOH** (Sh, Sh),¹² **4·CF₃SO₃·MeOH** (Sh),¹⁴ **4-PF₆·1.5H₂O** (Sh),⁷ **4·N(SO₂CF₃)₂** (Sh),¹⁵ **5·Cl·MeCN·H₂O** (Sh, Sh)¹⁶) reveals that all crystal packings look roughly similar with strong interchain DD interactions ($\text{Qn}\cdots\text{Qn}$) and relatively modest interlayer DD interactions ($\text{Ph-X}\cdots\text{Ph-X}$ or $\text{Qn}\cdots\text{Ph}$). This supramolecular arrangement is observed in compounds with very different anions regarding their composition, volume and geometry.

It is important to mention that the differences in solvating molecules were expected to have a greater impact on the cooperativity with a special emphasis on the interlayer interactions. In fact, what we observed is that the solvent molecules are usually only bounded to one cation molecule, which greatly diminishes their impact in intrachain, interchain or interlayer DD connectivities. This result contradicts the established view, many times referred in several publications, where a simple solvent change in the solid structure is responsible for a dramatic change in magnetic behavior. Our interpretation is that the key structural alteration induced by modifications of the solvating molecules might not be the differences in the cation–solvent interactions, but all the modulation of the interchain and interlayer interactions that occurs when the solid structure accommodates a new solvating molecule.

The critical aspect to control the sharpness of the SCO transition in these compounds seems to be directly related to the control, in the solid structure, of the degree of interchain and interlayer interactions. To obtain sharp transitions, it is necessary to maximize the interchain interactions and minimize the interlayer interactions. The chemical design of these systems will necessarily need to take this information into account and all chemical modification introduced into the compounds should always aim to maximize DD interchain connectivity at the same time as it minimizes interlayer interactions promoted by either DD, DAD interactions.

Conclusions

The structural differences that control the sharpness of the SCO transition in a set of Fe^{III} compounds was analyzed. This sharpness corresponds to the physical representation of the



cooperativity of the system. The supramolecular configuration in the studied compounds consists in arrangements of parallel layers of chains of cations with very strong cation–cation intrachain interactions, strong interchain cation–cation (intralayer) interactions and weak interlayer cation–cation interactions. This study showed that the intrachain interactions do not change in the studied compounds, being the strongest type of supramolecular interactions present. We were able to identify two factors that can independently contribute to the enhancement of the cooperativity and consequently to the enhancement of the sharpness of the SCO transition. The cooperativity is enhanced with the reinforcement of the interchain interactions and with the weakening of the interlayer interactions. These factors can be modulated separately or in conjunction to modify the cooperativity of the compound.

The modification of the interchain interactions can be obtained by tuning the cation–cation interactions. This tuning results from differences in the cation layer packing and is heavily dependent on the aromatic fragment (quinoline) interactions. The degree of interactions is not directly proportional to the volume of the substituent X used in the ligand 5-X-qsal.

The modification of the interlayer interactions can be obtained *via* two different mechanisms: the alteration of the direct cation–cation interlayer interactions or the mediated cation–anion–cation interactions. Both structural modifications appear to contribute equally to the modulation of the sharpness of the transition.

It is worth mentioning that in the studied compounds no phase transitions are associated with the spin transition. In fact if a structural transition takes place in a compound the conclusions of the present study might not apply to it, depending on the structural modifications that the transition induces.

The intelligent design of these materials should aim to synthesize compositions that maximize in the solid structure the cation–cation interactions within each chain and layer as much as possible and at the same time minimize the interlayer connectivity considering both cation–cation and cation–anion–cation interactions.

Author contributions

Conceptualization, B. J. C. V., L. C. J. P., V. d. G. and J. C. W.; methodology, B. J. C. V., L. C. J. P., V. d. G. and J. C. W.; validation, B. J. C. V., L. C. J. P., V. d. G. and J. C. W.; formal analysis, B. J. C. V., L. C. J. P., V. d. G. and J. C. W.; investigation, B. J. C. V., L. C. J. P., V. d. G. and J. C. W.; resources, B. J. C. V., L. C. J. P., V. d. G., and J. C. W.; writing – original draft preparation, B. J. C. V., L. C. J. P., V. d. G. and J. C. W.; writing – review and editing, B. J. C. V., L. C. J. P. and J. C. W.; supervision B. J. C. V., L. C. J. P., V. d. G. and J. C. W.; project administration, B. J. C. V. and J. C. W. All authors have read and agreed to the published version of the manuscript.

Conflicts of interest

There are no conflicts to declare.

Acknowledgements

This research was funded by FCT, Fundação para a Ciência e a Tecnologia, I.P., contracts PTDC/QUI-QIN/32240/2017, UID/Multi/04349/2019 and LTHMFL-NECL LISBOA-01-0145-FEDER-022096.

References

- P. Gütllich and H. A. Goodwin, Spin Crossover—An Overall Perspective, *Top. Curr. Chem.*, 2004, vol. 233, pp. 1–47.
- M. A. Halcrow, *Spin-Crossover Materials: Properties and Applications*, John Wiley & Sons, Ltd., Chichester, UK, 2013.
- P. Koningsbruggen, Y. Maeda and H. Oshio, *Spin Crossover in Transition Metal Compounds I*, ed. P. Gütllich and H. A. Goodwin, Springer, Berlin/Heidelberg, Germany, 2004, vol. 233, pp. 259–324.
- T. Shiga, R. Saiki, L. Akiyama, R. Kumai, D. Natke, F. Renz, J. M. Cameron, G. N. Newton and H. A. Oshio, Brønsted-Ligand-Based Iron Complex as a Molecular Switch with Five Accessible States, *Angew. Chem., Int. Ed.*, 2019, **58**, 5658–5662.
- I.-R. Jeon, C. Mathonière, R. Clérac, M. Rouzières, O. Jeannin, E. Trzop, E. Collet and M. Fourmigué, Photoinduced reversible spin-state switching of an Fe^{III} complex assisted by a halogen-bonded supramolecular network, *Chem. Commun.*, 2017, **53**, 10283–10286.
- W. Phonsri, D. S. Macedo, K. R. Vignesh, G. Rajaraman, C. G. Davies, G. N. L. Jameson, B. Moubaraki, J. S. Ward, P. E. Kruger and G. Chastanet, *et al.*, Halogen Substitution Effects on N₂O Schiff Base Ligands in Unprecedented Abrupt Fe^{II} Spin Crossover Complexes, *Chem. – Eur. J.*, 2017, **23**, 7052–7065.
- B. J. C. Vieira, L. C. J. Pereira, V. D. Gama, I. C. Santos, A. C. Cerdeira and J. C. Waerenborgh, Correlation between Supramolecular Connectivity and Magnetic Behaviour of [Fe^{III}(5-X-qsal)₂]⁺-Based Salts Prone to Exhibit SCO Transition, *Magnetochemistry*, 2022, **8**, 1.
- K. Takahashi, T. Sato, H. Mori, H. Tajima and O. Sato, Correlation between the magnetic behaviors and dimensionality of intermolecular interactions in Fe(III) spin crossover compounds, *Phys. B*, 2010, **405**, S65–S68.
- H. Oshio, K. Kitazaki, J. Mishiro, N. Kato, Y. Maeda and Y. Takashima, New spin-crossover iron(III) complexes with large hysteresis effects and time dependence of their magnetism, *J. Chem. Soc., Dalton Trans.*, 1987, 1341–1347.
- S. Hayami, K. Hiki, T. Kawahara, Y. Maeda, D. Urakami, K. Inoue, M. Ohama, S. Kawata and O. Sato, Photo-Induced Spin Transition of Iron(III) Compounds with π - π Intermolecular Interactions, *Chem. – Eur. J.*, 2009, **15**, 3497–3508.
- W. Phonsri, D. J. Harding, P. Harding, K. S. Murray, B. Moubaraki, I. A. Gass, J. D. Cashion, G. N. L. Jameson and H. Adams, Stepped spin crossover in Fe(III) halogen substituted quinolylsalicylaldehyde complexes, *Dalton Trans.*, 2014, **43**, 17509–17518.



- 12 D. J. Harding, W. Phonsri, P. Harding, K. S. Murray, B. Moubaraki and G. N. L. Jameson, Abrupt two-step and symmetry breaking spin crossover in an iron(iii) complex: An exceptionally wide [LS-HS] plateau, *Dalton Trans.*, 2015, **44**, 15079–15082.
- 13 W. Phonsri, P. Harding, L. Liu, S. G. Telfer, K. S. Murray, B. Moubaraki, T. M. Ross, G. N. L. Jameson and D. J. Harding, Solvent modified spin crossover in an iron(iii) complex: Phase changes and an exceptionally wide hysteresis, *Chem. Sci.*, 2017, **8**, 3949–3959.
- 14 D. J. Harding, W. Phonsri, P. Harding, I. A. Gass, K. S. Murray, B. Moubaraki, J. D. Cashion, L. Liu and S. G. Telfer, Abrupt spin crossover in an iron(iii) quinolylsalicylaldimine complex: Structural insights and solvent effects, *Chem. Commun.*, 2013, **49**, 6340–6342.
- 15 N. Phukkaphan, D. L. Cruickshank, K. S. Murray, W. Phonsri, P. Harding and D. J. Harding, Hysteretic spin crossover driven by anion conformational change, *Chem. Commun.*, 2017, **53**, 9801–9804.
- 16 D. J. Harding, D. Sertphon, P. Harding, K. S. Murray, B. Moubaraki, J. D. Cashion and H. Adams, Fe^{III} Quinolylsalicylaldimine Complexes: a rare mixed-spin-state complex and abrupt spin crossover, *Chem. – Eur. J.*, 2013, **19**, 1082–1090.

